Journal of Controlled Release 365 (2024) 412–421

Contents lists available at ScienceDirect

Journal of Controlled Release

journal homepage: www.elsevier.com/locate/jconrel

Review article

Targeting diffuse midline gliomas: The promise of focused ultrasound-mediated blood-brain barrier opening

Payton J. Martinez [a,b,*], Adam L. Green [c], Mark A. Borden [a,b]

[a] Biomedical Engineering Program, University of Colorado Boulder, Boulder, CO 80303, United States
[b] Department of Mechanical Engineering, University of Colorado Boulder, Boulder, CO 80303, United States
[c] Morgan Adams Foundation Pediatric Brain Tumor Research Program, Department of Pediatrics, University of Colorado School of Medicine, Aurora, CO 80045, United States

ARTICLE INFO

Keywords:
Diffuse midline gliomas
Focused ultrasound
Microbubbles
Drug delivery
State of the art

ABSTRACT

Diffuse midline gliomas (DMGs), including diffuse intrinsic pontine glioma, have among the highest mortality rates of all childhood cancers, despite recent advancements in cancer therapeutics. This is partly because, unlike some CNS tumors, the blood-brain barrier (BBB) of DMG tumor vessels remains intact. The BBB prevents the permeation of many molecular therapies into the brain parenchyma, where the cancer cells reside. Focused ultrasound (FUS) with microbubbles has recently emerged as an innovative and exciting technology that non-invasively permeabilizes the BBB in a small focal region with millimeter precision. In this review, current treatment methods and biological barriers to treating DMGs are discussed. State-of-the-art FUS-mediated BBB opening is then examined, with a focus on the effects of various ultrasound parameters and the treatment of DMGs.

1. Introduction

In 1926, Wilfred Harris first described diffuse intrinsic pontine glioma (DIPG) as an important tumor affecting the pontine area of the brain stem. DIPG remains one of the most difficult brain tumors to treat [1]. Through genetic sequencing of biopsies and autopsies from patients, it has been shown that over 80% of DIPG have a similar somatic gain-of-function mutation, where a missense substitution of lysine 27 to methionine in either histone variant HIST1H3B (H3.1) or H3F3A (H3.3), is found [2–4]. The World Health Organization (WHO) recently classified DMGs with this mutation as "diffuse midline glioma, H3 K27M-altered" [5]. Thus, a distinction was made with DMGs that lack the H3K27M mutation, although they may still exhibit a loss of the H3K27 trimethylation [5]. The proposed mechanism behind this variation is the overexpression of EZH inhibitory protein, which acts similarly to the K27M mutation that inhibits the polycomb repressive complex 2 [6,7]. With this information, considerable research has been done to find targetable epigenetic modifiers. These strategies include EZH2 inhibitors [8,9], histone deacetylase inhibitors [10,11], and H327 demethylase or methyltransferase inhibitors to target trimethylation [12]. Novel drugs have been developed to target and regulate the immune system's contribution to the tumor microenvironment [13,14]. However, many of these drugs cannot permeate the tumor BBB. Focused ultrasound complemented with microbubbles (MBs) has materialized as a promising non-invasive technique for opening the BBB temporarily. This review summarizes the obstacles associated with DMG treatments, examines the use of MB-mediated FUS to provide a noninvasive means to treat DMGs, and proposes further research on MB + FUS to treat DMGs with greater safety and efficacy.

1.1. DIPG overview

DIPG is mainly diagnosed in children, with the most common incidence at 6 to 9 years old [15–17]. A similar distribution is found between males and females [16]. Currently, DIPG accounts for 80% of all brainstem tumors [18]. Even though DIPG is prominent, with approximately 200–400 children diagnosed each year in the United States [19], the median survival has remained only 8–12 months, with under 10% of all patients surviving two years past their diagnosis date [20]. DIPG typically comprises at least 50% of the pons. The pons sits in the middle of the brainstem between the midbrain, medulla, and cerebellum [21]. The pons' function is divided at the coronal plane. The pontine tegmentum (dorsal pons) contains cranial nerve nuclei (CN V-VIII) and their associated tracts and is responsible for bridging the gap between

* Corresponding author at: 1111 Engineering Drive, Boulder, CO 80309, United States.
E-mail address: payton.martinez-1@colorado.edu (P.J. Martinez).

https://doi.org/10.1016/j.jconrel.2023.11.037
Received 10 August 2023; Received in revised form 13 November 2023; Accepted 18 November 2023
Available online 30 November 2023
0168-3659/Published by Elsevier B.V.

the medulla and thalamus [21–23]. The basis pontis (ventral pons) contains the white matter fibers of the corticospinal tract connecting the cerebral cortex to the spinal cord [21,23]. Therefore clinical symptoms often include cranial neuropathies and ataxia [24,25].

2. Current treatments of DIPG

The location and diffuse nature of DIPG make resection impossible. For over 50 years now, the most common treatment has remained radiation therapy. Photon therapy only marginally improves survival by an average of 3 months at the recommended dose of 54 Gy over 6 weeks [16,26]. As treatments have become more targeted, neuroaxis (axis of the CNS) spread has become more prevalent. Beyond radiation therapy, clinical trials have been done to test the ability of various chemotherapeutics to treat DIPG more effectively. Some of these clinical trials are summarized in Table 1. Each therapeutic targets a different aspect of DIPG biology, including epigenetics, cell metabolism, cellular signaling, DNA repair, and the cell cycle. The main class of chemotherapeutics that have been used to treat DIPG include HDAC inhibitors (panobinostat, vorinostat), proteasome inhibitors (marizomib, bortezomib), kinase inhibitors (ribociclib), topoisomerase II inhibitors (etoposide). Unfortunately, none of these clinical trials have shown an improvement in survival. Lin et al. conducted a large screening of all clinical chemotherapeutics, proteasome, and HDAC inhibitors where they found that panobinostat and marizomib showed the most promise in combination [27]. During this study drugs were ranked based on their ability to bypass the BBB. The limitation put on these drugs has led many groups to turn to drug delivery methods. There are three major methods to achieve this: convection-enhanced delivery (CED), nanoparticles, and chemical disruption of the BBB.

2.1. Issues with current treatments

One major obstacle to the efficacy of current treatments is the low accumulation of chemotherapeutic drugs in the tumor region. Similar to other regions of the brain, the pons, where DIPG is located, has an intact blood-brain barrier that prevents drugs from entering the parenchyma. One current approach to address this issue is convection-enhanced delivery (CED). CED involves the insertion of a catheter or catheters through the skull into the pons region, from which drugs are pumped using positive pressure and an engineered catheter tip to enhance fluid flow and convective mass transport into the surrounding tissue [28,29]. This method has shown higher therapeutic concentrations at the target site with less systemic toxicity [28,29]. However, CED has a few problems, especially in the treatment of solid tumors. Many tumors are highly vascularized and therefore are less susceptible to the positive pressure-driven flow [30]. Additionally, quickly growing tumors can develop areas of necrosis, in which CED is less effective as drugs can pool in this area preventing delivery to the faster-growing cells on the periphery [31]. Of course, the invasiveness of this technique is also a

Table 1
Table showing all clinical trials started since 2020 involving the delivery of chemotherapeutics to patients with DIPG or DMG. Highlighted rows show trials using focused ultrasound or convection-enhanced delivery. Data was obtained from clincaltrials.gov on May 10th, 2023.

Title	NCT Number	Status	Interventions	Phase	Start Date	Location
A Study of Low Dose Bevacizumab With Conventional Radiotherapy Alone in DIPG	NCT04250064	Recruiting	Drug: Bevacizumab Radiation: Ultra-low-dose RT	2	4-Feb-20	Tata Memorial Hospital, Mumbai, Maharashtra, India
INCB7839 in Treating Children With Recurrent/Progressive High-Grade Gliomas	NCT04295759	Recruiting	Drug: INCB7839	1	27-Jul-20	Children's Hospital Los Angeles, Los Angeles, California, United States…
Phase I Study of Marizomib + Panobinostat for Children With DIPG	NCT04341311	Active, not recruiting	Drug: Marizomib/ Panobinostat	1	10-Aug-20	Boston Children's Hospital, Boston, Massachusetts, United States…
A Study of BXQ-350 in Children With Newly Diagnosed DIPG or DMG	NCT04771897	Recruiting	Drug: BXQ-350	1	24-May-21	Children's Hospital Colorado, Aurora, Colorado, United States...
Non-Invasive Focused Ultrasound (FUS) With Oral Panobinostat in Children With Progressive DMG	NCT04804709	Active, not recruiting	Drug: Panobinostat Device: FUS with neuro-navigator-controlled sonication	1	28-Jul-21	Columbia University Irving Medical Center / New York-Presbyterian Hospital, New York, New York, United States
ONC206 for Treatment of Newly Diagnosed, or Recurrent Diffuse Midline Gliomas, and Other Recurrent Malignant CNS Tumors	NCT04732065	Recruiting	Drug: ONC206 Radiation: RT	1	23-Aug-21	University of California, San Francisco, San Francisco, California, United States; University of Michigan, Ann Arbor, Michigan, United States…
Combination Therapy for the Treatment of DMG	NCT05009992	Recruiting	Drug: ONC201 / Paxalisib Radiation: RT	2	20-Oct-21	University of Alabama at Birmingham, Birmingham, Alabama, United States…
CBL0137 for the Treatment of Relapsed or Refractory Solid Tumors, Including CNS Tumors and Lymphoma	NCT04870944	Active, not recruiting	Drug: FACT Complex-targeting Curaxin CBL0137	1/2	18-Jan-22	Children's Hospital of Alabama, Birmingham, Alabama, United States; Children's Hospital Los Angeles, Los Angeles, California, United States…
A Study of the Drug Selinexor With Radiation Therapy in Patients With Newly-Diagnosed DIPG and HGG	NCT05099003	Recruiting	Procedure: Biopsy / MRI Radiation: RT Drug: Selinexor	1/2	5-May-22	Children's Hospital of Alabama, Birmingham, Alabama, United States; Banner Children's at Desert, Mesa, Arizona, United States…
A Phase 1/2 Study of Sonodynamic Therapy Using SONALA-001 + Exablate 4000 Type 2 in Patients With DIPG	NCT05123534	Recruiting	Combination Product: SONALA-001 (ALA) and MR-Guided Focused Ultrasound device	2	12-Aug-22	Ivy Brain Tumor Center, Phoenix, Arizona, United States; University of California, San Francisco, San Francisco, California, United States…
A Drug-drug Interaction Study of Avapritinib and Midazolam	NCT04908176	Recruiting	Drug: Avapritinib / midazolam	1	24-Aug-22	Mayo Clinic Florida, Jacksonville, Florida, United States…
Biological Medicine for DIPG Eradication 2.0	NCT05476939	Recruiting	Drug: Everolimus/ ONC201 Radiation: RT	3	29-Sep-22	Gustave Roussy, Villejuif, Val De Marne, France…
Oral AMXT 1501 Dicaprate in Combination With IV DFMO	NCT05500508	Recruiting	Drug: AMXT1501 / DFMO	1/2	29-Nov-22	Cincinnati Children's Hospital Medical Center, Cincinnati, Ohio, United States…
BBB Disruption Using Exablate FUS With Doxorubicin for Treatment of Pediatric DIPG	NCT05615623	Recruiting	Device: Exablate Drug: Doxorubicin	1/2	4-Jan-23	Sunnybrook Research Institute, Toronto, Ontario, Canada
BBB Disruption Using Exablate FUS With Doxorubicin for Treatment of Pediatric DIPG	NCT05630209	Recruiting	Device: Exblate Drug: Doxorubicin	1/2	Feb-23	Children's National Medical Center, Washington, District of Columbia, US
131I-omburtamab Delivered by Convection-Enhanced Delivery in Patients With DIPG	NCT05063357	Not yet recruiting	Drug: 131I-Omburtamab Device: CED	1	Mar-23	N/A
FUS Etoposide for DMG - A Feasibility Study	NCT05762419	Recruiting	Drug: Etoposide (Oral) Device: FUS with neuro-navigator-controlled sonication	1	Mar-23	Columbia University Irving Medical Center, New York, New York, United States
Loc3CAR: Locoregional Delivery of B7-H3-CAR T Cells for Pediatric Patients With Primary CNS Tumors	NCT05835687	Recruiting	Drug: B7-H3-CAR T cells	1	25-Apr-23	St. Jude Children's Research Hospital, Memphis, Tennessee, United States
Study of Ribociclib and Everolimus in HGG and DIPG	NCT05843253	Not yet recruiting	Drug: Ribociclib / Everolimus	2	15-Aug-23	Children's Hospital Colorado, Aurora, Colorado, United States…

DIPG = diffuse intrinsic pontine glioma; CED = convection-enhanced delivery; FUS = Focused Ultrasound; HGG = High-Grade Glioma; BBB = Blood-Brain Barrier; RT = Radiation Therapy.

concern, as it requires stereotactic surgery to place the catheter(s). Clinical trials have shown the potential for an increase in neurological issues at CED higher flow rates [32].

Nanoparticles have become a common method to deliver drugs across the BBB. Nanoparticles are modular, allowing for the engineering of various characteristics to utilize specific biological mechanisms. Nanoparticles have been used successfully to deliver drugs into solid tumors [33,34]. Nanoparticles can be engineered to cross the BBB via different pathways, including endocytosis or transcytosis (active transport using a surface receptor) and the enhanced permeability and retention (EPR) effect [35]. Once past the BBB, nanoparticles release their drug cargo into the tissue extracellular matrix (where they can be taken up by the cells) or directly into the cytoplasm of the target cells. Although nanoparticles have shown promising effects in animal models, there has been little success in human clinical trials because they cannot reach the minimal effective dose within the tumor interstitium [34,36]. Since nanoparticle accumulation may depend on the EPR effect, they may require the BBB to be opened for drug accumulation to be observed. While many gliomas have leaky vessels, DIPG, and several other high-grade gliomas have an intact blood-brain barrier. Overall, nanoparticle technology could be significantly improved if methods are developed to open the BBB noninvasively, locally, and transiently [37,38].

Other ways groups have tried to disrupt the BBB is through intra-arterial vasoactive agents that cause an inflammatory reaction in the endothelial cells. One class of these drugs is alkylglycerols which can temporarily destabilize the cell membrane of endothelial cells, opening the BBB between 3 and 15 min [39]. Although these methods have had great success at increasing the delivery of large-molecule drugs, their non-selectivity to the tumor site causes problems when the chemotherapeutic is also toxic to health cells. Bradykinin and its analog RMP-7 are more specific to some tumor types that overexpress the B_2 receptor [40]. Although RMP-7 was not shown to be effective with lipophilic chemotherapies. When taken to clinical trials in combination with carboplatin, which showed effectiveness in rats, the study was shown to be ineffective [41].

2.1.1. The blood brain barrier (BBB)

As previously discussed, one major hurdle for drug delivery to DIPG and other neurological diseases is the BBB [42,43], which serves as a defense against harmful chemicals or biological agents. The BBB is tightly regulated by the vascular system of the brain and comprises highly polarized endothelial cells that are firmly connected via tight junctions. These tightly bound endothelial cells are surrounded by pericytes and astrocytic foot processes, which further contribute to the barrier function [44,45] (Fig. 1). The astrocytic end feet cover around 99% of all capillaries in the brain and are vital in regulating the extracellular matrix (ECM) composition surrounding the endothelial cells [46]. They also regulate the amount of immune cell infiltration and the integrity and permeability of the BBB [46,47]. Pericytes are one of the main supporting cells that regulate vessel formation and growth [36,48]. All three, astrocytic end feet, pericytes, and tightly joined endothelial cells surround the basal lamina that consists of an ECM and provides a space for regulation of the molecular transport [36]. Within the endothelium, the tight junctions in conjunction with adherence proteins (occludins, tricellulins, claudins, and junctional adhesion molecules) prevent paracellular diffusion of large (400 Da) molecules [48,49]. Therefore, any therapeutics needing to enter the brain must pass through the luminal plasma membrane of these endothelial cells. Some endothelial cells contain efflux transporters that allow the movement of substrates into the parenchyma [50]. Therefore, to pass through the BBB, drugs must be engineered with the following properties: high lipophilicity, low molecular mass, low hydrogen bonding potential, and noninteraction with efflux transporters. Once past the BBB, molecular drugs or drug-loaded nanoparticles must contend with microglia, which are the main immune cells within the brain parenchyma [51,52].

2.1.2. Blood-brain tumor barrier (BBTB)

In some CNS tumors, the integrity of the blood-brain tumor barrier (BBTB) is often disrupted either biochemically or physically. The use of magnetic resonance imaging (MRI) using a gadolinium-based contrast agent is the most common way to confirm BBB disruption, as these contrast agents are normally unable to pass the BBB or BBTB. This disruption usually occurs at the center of the tumors, where the interstitial pressure is greater, while the BBB in the margins remains intact. This phenomenon has led to incomplete tumor reduction, where malignant tumor cells can develop through other parts of the brain [53]. In contrast to some CNS tumors, which demonstrate a leaky BBTB, DMGs in particular do not possess this quality [54–56]. An impermeable BBTB also limits the tumor margin visibility on T1-weighted contrast-enhanced MRI scans, which can make it difficult to diagnose the early stages of tumor growth [57]. Moreover, the pons and brainstem possess a more unyielding BBTB, further complicating the penetration of pharmaceuticals [58]. A study by McCully et al. showed that the BBTB is inhomogeneous, as there was a difference in temozolomide penetration between the brainstem region and the cortex [58]. Like other CNS tumors, DMG can show some enhancement at the center of the tumor illustrating necrosis. Some studies have shown decreased BBTB permeability due to an upregulated Sonic Hedgehog (SHH) signaling [59]. SHH is from the Hedgehog family of morphogens that orchestrates

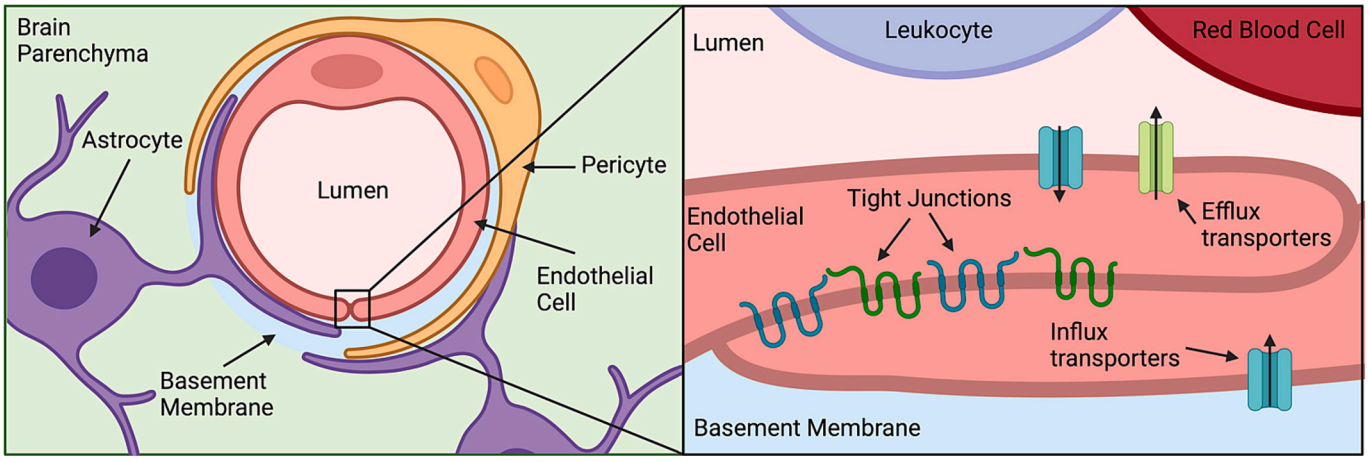

Fig. 1. Cartoon of the blood-brain barrier. The left image shows a single neurovascular unit. The right shows an in-depth view of tight junctions and endothelial surface transporters.

branching morphogenesis and therefore vascularization. Other groups have shown the presence of P-glycoprotein/MDR1 (P-gp), and Breast Cancer Resistance Protein 1 found directly on DIPG cells on both the glioma cells and surrounding tissue [60]. P-gp can reduce drug accumulation within cells by actively removing drugs using ATP [61]. Deligne et al. studied in vitro models of the DIPG BBB to determine the reason for its chemoresistance. The authors found over a week of DIPG cell development no change in the integrity of the drug penetration or the amount of efflux transporters [56]. However, we still do not have direct evidence of why the BBTB in DIPG presents differently than for healthy tissue in vivo.

3. Focused ultrasound meditated blood-brain barrier opening

Focused ultrasound (FUS) complemented with microbubbles (MBs) has materialized as a non-invasive technique to momentarily open the BBB [62–65]. MBs utilized for this technique were originally developed as ultrasound contrast agents. They are 1–10 um in diameter, with a shell (typically lipid or protein) that encapsulates a high-molecular-weight internal gas (e.g., perfluorocarbons) [66–68]. The physical mechanism that has been proposed is that circulating microbubbles are forced to expand and contract (cavitate) under ultrasound (0.2–2 MHz). As a result, the local mechanical forces cause the separation of tight junctions, opening the BBB [69,70]. Two types of cavitation can occur: harmonic and inertial. Harmonic cavitation is characterized by small oscillations of the microbubble and can produce an acoustic response at regular fractions and multiples of the driving frequency [71,72]. Harmonic (specifically the sub and ultra-harmonic) responses are caused by the nonlinear and asymmetric response of the microbubbles as they expand and contract [71]. Inertial cavitation can be described by violent expansion and contraction, eventually reaching the critical point of implosion, shock wave formation, and production of a broadband acoustic frequency response [71,72]. Both regimes of cavitation produce mechanical forces (e.g., fluid shear, shock waves, and micro-jetting) to the endothelium within the focal zone of the FUS, causing disruption of the bonds between the tight junction proteins [71,72]. FUS-mediated BBB opening is safe with no significant neuronal damage, apoptosis, ischemia, or longer-term damage to the vessels [63]. Localized BBB opening can remain for a period of 3 to 24 h, depending on the intensity of the focused ultrasound [73]. The reversibility of BBB opening, and the small focal zone makes MB + FUS a good candidate for targeted delivery of drugs that cannot otherwise pass the BBB.

Beyond the initial effects of BBB opening, a cascade of events occurs along with the opening. First, there is a resulting immune response from opening the BBB. Previous work has shown that FUS-mediated BBB opening can induce sterile inflammation [74]. This may also contribute to the recruitment of active T cells to the site, leading to a strong immune infiltration into tumors [75]. Microglia can also respond to any damage to the vascular system by releasing inflammatory cytokines and vascular growth factors [52,76]. Secondly, FUS has been shown to suppress the Pgb (P-glycoprotein) transporter found in endothelial cells making up the BBB by 50–60% [77,78]. As previously discussed, this multidrug resistance protein can also be present in DIPG tumors and can lead to resistance to chemotherapeutics. Therefore, the use of FUS-mediated drug delivery may also reduce the risk of resistance and increase the drug concentrations in these tumors.

3.1. Using focused ultrasound to deliver drugs to DIPG tumors

In 2001, Hynynen et al. first showed that BBB opening was possible in a rabbit using MB + FUS [62]. Since then, we have seen the field rapidly expand to encompass a variety of neurological diseases in several animal models and humans. Within the past decade, there has been an interest in using MB + FUS to better target and treat tumors that are located in non-resectable areas of the brain. Among these, DIPG has stood out as a prime candidate for this technology due to its diffuse and intrinsic nature. These preclinical studies are summarized in Table 2.

3.2. Characterization of FUS-induced BBB opening, and agents used

As FUS-meditated BBB opening has developed, there has been a wide range of therapeutics developed with this method. Smaller chemotherapeutic drugs that range from 150 Da to 1 kDa have been delivered, including BCNU (Carmustine) [64,85–87], cisplatin [79], etoposide [88,89], irinotecan [90], carboplatin [91], and doxorubicin [79,92–95]. Larger therapeutics delivered by MB + FUS include antibodies, viruses, nanoparticles, and protein-based therapeutics, such as trastuzumab (Herceptin), pertuzumab [96–98], adeno-associated virus (AAV) [99], the immunomodulating agent IL-12 [100], and ^{68}Ga-labeled bevacizumab (Avastin) (a humanized antiangiogenic monoclonal antibody) [101]. These molecules range from 70 to 150 kDa. Overall, there has been great success in the delivery of even the largest therapeutics, showing the versatility of MB + FUS as a drug delivery mechanism. However, due to the different drug administration methods (intraperitoneally, intravenously, etc.), we are unable to directly compare extravasation across all studies.

Most studies use MRI confirmation and quantification of the extent of BBB opening. As stated earlier, MRI is used with gadolinium-based contrast agents for T1-weighted imaging. Table 3 shows these contrast agents and their molecular weights. Most of the contrast agents range from 510 to 950 Da when not bound to serum proteins. Those that do not bind are relevant for small-molecule drug kinetics. MR contrast agents that strongly bind to serum proteins can provide insight into how larger drug molecules and particles may pass through the BBB (represented in Table 3 by a *). Nuclear imaging using radioactive isotopes can also be used to track molecules moving past the BBB. The two main modalities are positron emission tomography (PET) and Single-photon emission computerized tomography (SPECT). Nuclear imaging has a variety of radiopharmaceuticals that can show different aspects of BBB dysfunction including [^{68}Ga]DTPA and [^{68}Ga]EDTA for BBB opening, [^{18}F]FDG for glucose transport, and [^{11}C]Verapamil and [^{11}C]Loperamide for p-gp transport. For a more comprehensive list of PET tracers for P-gp, we refer to Syvänen and Eriksson [102] and for their use particularly with FUS-mediated BBBO, we refer to Arif et al. [103]. All of these radiopharmaceuticals can also be seen in Table 3. Fluorescently labeled dextrans and liposomes with a wide range of molecular weights have been used to mimic drug extravasation past the BBB [104–106], although this must be determined ex vivo. Evans blue dye is the most common ex vivo marker of BBB opening. Other fluorescent dyes can be used that are not as toxic as Evans Blue [107].

3.3. FUS technology and sonication parameters

FUS has a wide variety of parameters, including frequency, pressure amplitude, pulse waveform, pulse length, and pulse repetition frequency, that relate to its energy applied over time. Table 2 shows the reported technical specifications for each study employing FUS-mediated drug delivery to DIPG tumors. The most widely used metric to determine the extent of BBB opening is the mechanical index (MI) due to its strong correlation to cavitation inception and inertial cavitation [127]. MI is a unifying ultrasound parameter that combines the ultrasound fundamental frequency (f in units of MHz) and peak negative pressure (PNP in units of MPa). The relationship is [128]:

$$MI = \frac{PNP}{\sqrt{f}}$$

Many of the preclinical systems use a single-element spherically focused transducer that ranges from 0.2 to 2 MHz in the pulse center frequency. This range of frequencies has been shown to effectively penetrate the skull of small animals (mice, rats, and rabbits) [79,88,89,65,130,131] and larger mammals (primates and humans) [132,133], allowing focusing within the brain.

Table 2
Table of FUS-mediated BBBD drug delivery studies that were specifically done to more effectively treat DIPG. *Pressure was increased at this increment until PCD data showed sub and ultra-harmonic response. NR means not reported in the literature.

Study (Year)	Animal Strain	Drug / Vehicle	FUS Parameters					Microbubble parameters			Results
			Frequency (MHz)	PNP (MPa)	PRF (Hz)	PL (ms)	Time (s)	Size (μm)	Dose	Type	
Alli et al. (2018) [79]	NSG mice	Doxorubicin (5 mg/kg)	1.68	0.25 + 0.025*	1	10	120	1–10	20 μl/kg	Definity	50-fold increase
Ye et al. (2018) [80]	C57BL/6 mice	40 kDa dextran (2 mg)	1.5	0.56	5	0.67	120	4–5	2.4E7 MBs	DSPC-PEG2000; PFB gas	3-fold increase in dextran intensity
Ishida et al. (2021) [81]	NSG mice	Doxorubicin (5 mg/kg)	1.78	NR	0.67	10	180	1–10	20 μl/kg	Definity	4-fold increase; no survival benefit
Englander et al. (2021) [82]	B6 mice	Etoposide (20 mg/kg)	1.5	0.7	5	10	120	1–10	200 μl	SonoVue / Definity	8-fold increase; no survival benefit
Haumann et al. (2022) [83]	Foxn1 mice	Doxorubicin (5 mg/kg)	1.5	0.2–0.4	NR	NR	160	1–10	60 μl	SonoVue	no survival benefit
Martinez et al. (2023) [84]	Nu/nu mice	Panobinostat (10 mg/kg)	1.5	0.615	1	10	180	3	25 μl/kg	DSPC-PEG40s; PFB gas	3-fold increase; prolonged survival from 21 to 31 days

Table 3
Model drugs used to determine BBB permeability during FUS-mediated BBBD. *MW moves 69 kDa when attached to albumin in the blood.

Agent	Imaging Modality	Molecular Weight (Da)	Dose	Translatable	Model Uses
MultiHance (Gd-BOPTA)	MR	513.5*	5.29 mg/kg	Yes	[108]
Omniscan (Gadodiamide)	MR	573.7*	0.2 mmol/kg	Yes	[74,88,89,109,110]
Gadovist (Gd-DO3A-butrol)	MR	604.7	0.1–0.125 mmol/kg	Yes	[79,90,91,111]
Dotarem (Gd-DOTA)	MR	753.9	50 μl	Yes	[106]
Magnevist (Gd-DTPA)	MR	938.0*	0.1–0.25 mmol/kg	Yes	[97,101,112,113]
[^{68}Ga] DTPA	PET	1502.3	30–50 MBq	Yes	[114,115]
[^{99}mTc] DTPA	SPECT	485.21	130–150 MBq	Yes	[114,115]
[^{18}F] FDG	PET	181.26	37 MBq	Yes	[116,117]
[^{11}C] Loperamide	PET	477.05	0.76 ± 0.3 nmol/kg	Yes	[102,118,119]
[^{11}C] Verapamil	PET	491.07	6–10 nmol	Yes	[102,118,120–123]
Evans Blue	Fluorescence	960.8*	2–100 mg/kg	No	[74,86,101,124–126]
Dextrans	Fluorescence	3-1000 k	Varies	No	[80,101]

Although pulse length and pulse reptation frequency have not received as much attention as peak negative pressure and frequency, they still play an important role in the energy delivered. Initially burst length alone was thought to have an effect on BBBO [130]. Later it was realized that there is an interplay between the two parameters. Choi et al. showed that there is a window of pulse repetition frequencies that had an effect on BBBO. Less than 0.1 Hz did not open the BBB, and above 10 Hz did not have a significant difference [134]. The same group also showed a similar trend with pulse length seeing a small amount of dextran delivery at pulse lengths as low as 0.033 ms and a saturation above 10 ms [134]. Recently Morse et al. showed that using rapid short-pulses to obtain a more uniform BBBO at lower MIs [135,136]. Lim Kee Chang et al. employed a pulse sequence of 5 μs long pulse and 1.25 kHz pulse repetition frequency for 10 ms then repeated with a frequency of 0.5 Hz [137]. The group was able to deliver model agents ranging from 3 kDa to 66.5 kDa at a relatively low pressure of 0.35 MPa [137].

Passive cavitation detectors (PCDs) provide valuable real-time feedback on the MB acoustic response. Within the past 5 years, many FUS systems have incorporated a PCD into their setup to either record microbubble response or to provide feedback to better tailor treatment intensities [138]. Using PCDs and high-frequency optical imaging of microbubbles under ultrasound, the threshold for inertial cavitation was found to be around 0.4 MI [71,91,131]. A feedback mechanism was first put in place to provide a better safety index, as inertial cavitation has been associated with an increased probability of vascular and tissue damage [139,140]. These closed-loop systems use data collected from the previous pulse to make any necessary changes on the next pulse. Between each pulse, analysis methods usually give a "cavitation dose" via a Fourier transform analysis [71,139]. Depending on the pulse length and pulse repetition frequency (also can be found in Table 2), there can be issues with the analysis method used between pulses. These include high computation power for extremely high pulse repetition frequencies and overly long pulses that can lead to over-saturated FFTs, making the diagnosis of inertial cavitation more difficult.

Given the range of parameters that can be used during FUS-mediated BBB opening, a variety of clinical devices are available. There are three types of clinical devices: implantable devices, MRI-guided, and neuronavigation-guided. Carthera's SonoCloud is a nine-transducer system that is implanted under the skull usually after a brain tumor resection [141]. Although DIPG patients rarely receive a tumor resection increasing the invasiveness of this treatment option. The major upside to this device is the removal of uncertainty with the skull. Normally simulations have to be run to account for the heterogeneity of the bone. Insightec's Exablate was initially built for treatment to other parts of the body although they have produced a system for the brain. This clinical system uses a helmet-shaped multielement (~1000) transducer to focus the beam through the skull to the tumor [142]. Due to the penetration through the bone, MRI guidance is necessary throughout the treatment. One downside to this system is the fixed skull pins needed to maintain head position. Given the young average age of DIPG patients, this may be a concern for procedures. Finally, the latest device to enter the clinical scene is NaviFUS [143], and Columbia University's TheraWave. Using infrared cameras tracking the position of the head and transducer, targeting can be achieved without a fixed head. Similar to Exablate, a simulation using previously obtained MRI or CT scans is required to accurately target regions in the brain. Overall, the neuronavigation system looks the most promising for the DMG community.

3.4. Microbubble parameters

The second half of this technology is the use of MBs to provide an acoustic amplification point for the ultrasound. There are two specific MB parameters that provide an estimation of BBB opening. The first and most straightforward metric is the dose injected during treatments. Table 2 also illustrates the microbubble doses given during each preclinical study completed using DIPG as the model. Song et al. have shown that BBB opening is not only dependent on the number of microbubbles injected, which previously had been the only metric used but also based on the size of microbubbles used [65]. Microbubble volume dose (MVD) is the unifying dose metric of microbubble number and size injected. MVD is calculated by taking the average volume of each microbubble in the injection sample and multiplying it by the concentration injected per kg of body weight [65]. Clinically approved microbubbles for contrast-enhanced ultrasound imaging have a range of recommended doses, as they are polydisperse in size distribution and exhibit significant vial-to-vial variability. Typical dose ranges used for MB + FUS range from 0.16 to 0.44 μl/kg (SonoVue and Definity respectively) [70,144]. There have only been a few studies looking into the effects of microbubble dose on BBB opening. McMahon et al. looked into the effects of microbubble dose on the inflammatory response post BBB opening [145].

Secondly, the microbubble composition is vital in its success and safety during BBB opening (Fig. 2). There are three main FDA-approved and commercially available microbubble compositions which include SonoVue (Bracco, Milan, Italy) DSPC lipid-shelled microspheres with an internal gas of sulfur hexafluoride; Definity (Lantheus Medical Imaging, USA) DPPC-shelled microspheres containing a perfluoropropane internal gas; and Optison (GE Healthcare, USA) albumin-shelled microspheres with perfluoropropane inside. Many groups also use engineered microbubbles [108,65,146,147]. Many of these MB formulations use similar compositions to the commercially available ultrasound contrast agent microbubbles, but they are tailored to the treatment, including the addition of drug within or on the bubble surface that can be released during sonication [86,148–150]. These microbubbles have also been shown to improve targeting by conjugating shells with peptides [151] or antibodies [86]. Oxsonics' SonoTran Particles are nanocups that were specifically engineered to be cavitation nuclei improving the effect of low-intensity focused ultrasound. Bing et al. have reported that the microbubble composition has an effect on both BBB opening and acoustic feedback through a passive cavitation detector [152]. Overall, there lacks cohesion in the current literature reporting of microbubble parameters, making it more difficult to correlate MB doses across studies. Dauba et al. recently published a review of contrast agents used for BBB opening, where this issue was more clearly illustrated [153]. More work is necessary to correlate MB composition, microstructure, and physical properties (such as size, shell elasticity and viscosity, and surface architecture) to in vivo performance.

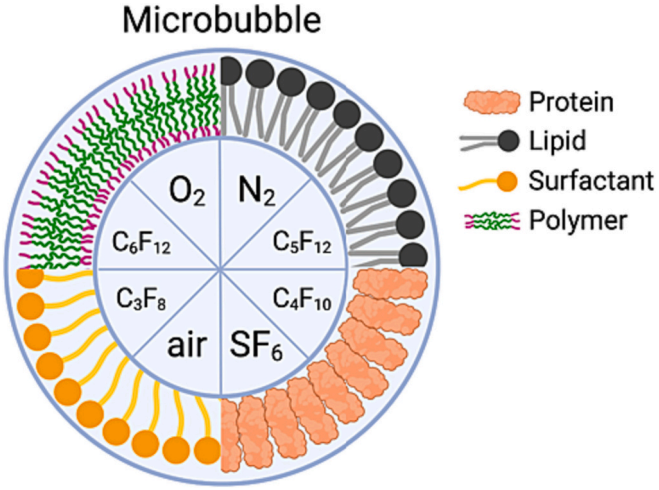

Fig. 2. Illustration of a variety of commonly used microbubble compositions.

3.5. Discussion of limitations and advantages of preclinical FUS

The use of FUS and MBs to temporarily open the blood-brain barrier has been shown to be an effective way to noninvasively increase the effectiveness of systemic drug delivery to a small focal region of the brain. As with any technology, there are limitations and advantages to this drug delivery method. These fit within three categories: ultrasound, microbubbles, and overall pathophysiology of the model.

Focused ultrasound parameters are a vital part of completing BBB opening safely and effectively. As previously discussed, lower frequencies (0.2 to 2 MHz) are primarily used during BBB opening for two reasons. First, the penetration through the skull is more effective at lower frequencies as the ultrasound wavelength is on the same length scale as the skull thickness (1 mm). Lower frequencies have also been associated with less microvasculature damage [130]. Staying within the lower frequency range, the mechanical index is a predictive metric for BBB opening, where it was found that at 0.46 MI the probability of opening was 50% [127]. A challenge remains where ultrasound parameters cannot be solely investigated, as we must also account for tissue damage, which increases as a function of MI. One way to account for acoustic pressure and MI is the use of PCD feedback control during treatments.

Microbubble parameters are also important and highly modular. Microbubbles can be controlled by manipulating composition, size, concentration, and infusion rate. The microstructure and properties of MBs can also be influenced by their synthesis method, processing history, storage conditions, and handling. For example, Definity microbubbles showed a wide range of size distributions solely based on their activation temperature [154]. Microbubbles can also degrade over time, eventually losing concentration and leading to a shift in the size distribution [71].

It is also important to consider the anatomy and physiology of the animal being treated. Most studies, in particular those studying DIPG, target regions within the brainstem. These tumors can have different vasculature than healthy brain tissue. Although we consider the BBB to remain intact for DMG, its location (most commonly pons and thalamus) has different vasculature than other brain regions (cortex, cerebellum). Furthermore, small animal models do not fully replicate brain anatomy in humans and therefore need to be carefully considered as research moves from preclinical models to the clinic [155].

4. Conclusion

Diffuse intrinsic pontine glioma is a very troubling disease that has had very few treatment options. One of the major challenges is the blood-brain barrier. Focused ultrasound-mediated blood-brain barrier opening with microbubbles is a modern image-guided way to effectively deliver drugs to a mm-scale spot in the brain, with excellent accuracy, precision, and control. There have been few preclinical studies treating DIPG using MB + FUS, and more work is needed to better define microbubble and ultrasound parameters to more effectively and safely treat DIPG.

Funding

This research was funded by the US National Institutes of Health, award R01CA239465, and the National Science Foundation award DGE 2040434.

CRediT authorship contribution statement

Payton Martinez: Writing – original draft, Visualization, Investigation, Conceptualization. **Adam L. Green:** Writing – review & editing, Supervision. **Mark A. Borden:** Writing – review & editing, Supervision, Funding acquisition.

Declaration of Competing Interest

The authors declare no conflict of interest.

Data availability

No data was used for the research described in the article.

Acknowledgements

Figures were in part made using Biorender.com.

References

[1] N.A. Vitanza, M. Monje, Diffuse intrinsic pontine glioma: from diagnosis to next-generation clinical trials, Curr. Treat. Options. Neurol. 21 (8) (2019) 37.
[2] D.A. Khuong-Quang, P. Buczkowicz, P. Rakopoulos, X.Y. Liu, A.M. Fontebasso, E. Bouffet, et al., K27M mutation in histone H3.3 defines clinically and biologically distinct subgroups of pediatric diffuse intrinsic pontine gliomas, Acta Neuropathol (Berl). 124 (3) (2012) 439–447.
[3] J. Schwartzentruber, A. Korshunov, X.Y. Liu, D.T.W. Jones, E. Pfaff, K. Jacob, et al., Driver mutations in histone H3.3 and chromatin remodelling genes in paediatric glioblastoma, Nature. 482 (7384) (2012) 226–231.
[4] St. Jude Children's Research Hospital–Washington University Pediatric Cancer Genome Project, Somatic histone H3 alterations in pediatric diffuse intrinsic pontine gliomas and non-brainstem glioblastomas, Nat. Genet. 44 (3) (2012) 251–253.
[5] D.N. Louis, A. Perry, P. Wesseling, D.J. Brat, I.A. Cree, D. Figarella-Branger, et al., The 2021 WHO classification of tumors of the central nervous system: a summary, Neuro-Oncol. 23 (8) (2021) 1231–1251.
[6] C. Antin, A. Tauziède-Espariat, M.A. Debily, D. Castel, J. Grill, M. Pagès, et al., EZHIP is a specific diagnostic biomarker for posterior fossa ependymomas, group PFA and diffuse midline gliomas H3-WT with EZHIP overexpression, Acta Neuropathol. Commun. 8 (1) (2020) 183.
[7] I.J. Findlay, G.N. De Iuliis, R.J. Duchatel, E.R. Jackson, N.A. Vitanza, J.E. Cain, et al., Pharmaco-proteogenomic profiling of pediatric diffuse midline glioma to inform future treatment strategies, Oncogene. 41 (4) (2022) 461–475.
[8] F. Mohammad, S. Weissmann, B. Leblanc, D.P. Pandey, J.W. Højfeldt, I. Comet, et al., EZH2 is a potential therapeutic target for H3K27M-mutant pediatric gliomas, Nat. Med. 23 (4) (2017) 483–492.
[9] K.M. Chan, D. Fang, H. Gan, R. Hashizume, C. Yu, M. Schroeder, et al., The histone H3.3K27M mutation in pediatric glioma reprograms H3K27 methylation and gene expression, Genes Dev. 27 (9) (2013) 985–990.
[10] C.S. Grasso, Y. Tang, N. Truffaux, N.E. Berlow, L. Liu, M.A. Debily, et al., Functionally defined therapeutic targets in diffuse intrinsic pontine glioma, Nat. Med. 21 (6) (2015) 555–559.
[11] N.A. Vitanza, M.C. Biery, C. Myers, E. Ferguson, Y. Zheng, E.J. Girard, et al., Optimal therapeutic targeting by HDAC inhibition in biopsy-derived treatment-naïve diffuse midline glioma models, Neuro-Oncol. 23 (3) (2021) 376–386.
[12] R. Hashizume, N. Andor, Y. Ihara, R. Lerner, H. Gan, X. Chen, et al., Pharmacologic inhibition of histone demethylation as a therapy for pediatric brainstem glioma, Nat. Med. 20 (12) (2014) 1394–1396.
[13] G.L. Lin, S. Nagaraja, M.G. Filbin, M.L. Suvà, H. Vogel, M. Monje, Non-inflammatory tumor microenvironment of diffuse intrinsic pontine glioma, Acta Neuropathol. Commun. 6 (1) (2018) 51.
[14] J.L. Ross, Z. Chen, C.J. Herting, Y. Grabovska, F. Szulzewsky, M. Puigdelloses, et al., Platelet-derived growth factor beta is a potent inflammatory driver in paediatric high-grade glioma, Brain. 144 (1) (2021) 53–69.
[15] C.R. Freeman, J.P. Farmer, Pediatric brain stem gliomas: a review, Int J Radiat Oncol. 40 (2) (1998) 265–271.
[16] T.B. Johung, M. Monje, Diffuse intrinsic pontine glioma: new pathophysiological insights and emerging therapeutic targets, Curr. Neuropharmacol. 15 (1) (2017) 88–97.
[17] K.L. Eschbacher, C.M. Ida, D.R. Johnson, M.A. Alvi, S.M. Jenkins, M.W. Ruff, et al., Diffuse gliomas of the brainstem and cerebellum in adults show molecular heterogeneity, Am. J. Surg. Pathol. 45 (8) (2021) 1082–1090.
[18] S.E. Veldhuijzen van Zanten, M.H. Jansen, E. Sanchez Aliaga, D.G. van Vuurden, W.P. Vandertop, G.J. Kaspers, A twenty-year review of diagnosing and treating children with diffuse intrinsic pontine glioma in the Netherlands, Expert Rev. Anticancer Ther. 15 (2) (2015) 157–164.
[19] Central Brain Tumor Registry of the United States, CBTRUS Statistical Report: Primary Brain and Central Nervous System Tumors Diagnosed in the United States in 2004–2006, 2023.
[20] P.G. Fisher, S.N. Breiter, B.S. Carson, M.D. Wharam, J.A. Williams, J.D. Weingart, et al., A clinicopathologic reappraisal of brain stem tumor classification: identification of pilocytic astrocytoma and fibrillary astrocytoma as distinct entities, Cancer. 89 (7) (2000) 1569–1576.
[21] S. Sciacca, J. Lynch, I. Davagnanam, R. Barker, Midbrain, pons, and medulla: anatomy and syndromes, RadioGraphics. 39 (4) (2019) 1110–1125.
[22] K. Gudmundsson, A.L. Rhoton, J.G. Rushton, Detailed anatomy of the intracranial portion of the trigeminal nerve, J. Neurosurg. 35 (5) (1971) 592–600.
[23] F. Chaddad-Neto, M.D. Silva da Costa, Surgical anatomy of the pons, in: Microneuroanatomy and Surgery [Internet], Springer International Publishing, Cham, 2022, pp. 177–198. Available from: https://link.springer.com/10.1007/978-3-030-82747-2_10.
[24] K.J. Cohen, N. Jabado, J. Grill, Diffuse intrinsic pontine gliomas—current management and new biologic insights. Is there a glimmer of hope? Neuro-Oncol. 19 (8) (2017) 1025–1034.
[25] L.M. Hoffman, S.E.M. Veldhuijzen van Zanten, N. Colditz, J. Baugh, B. Chaney, M. Hoffmann, et al., Clinical, radiologic, pathologic, and molecular characteristics of Long-term survivors of diffuse intrinsic pontine glioma (DIPG): a collaborative report from the international and European Society for Pediatric Oncology DIPG registries, J. Clin. Oncol. 36 (19) (2018) 1963–1972.
[26] K.J. Cohen, A. Broniscer, J. Glod, Pediatric glial tumors, Curr. Treat. Options Oncol. 2 (6) (2001) 529–536.
[27] G.L. Lin, K.M. Wilson, M. Ceribelli, B.Z. Stanton, P.J. Woo, S. Kreimer, et al., Therapeutic strategies for diffuse midline glioma from high-throughput combination drug screening, Sci. Transl. Med. 11 (519) (2019) eaaw0064.
[28] R.H. Bobo, D.W. Laske, A. Akbasak, P.F. Morrison, R.L. Dedrick, E.H. Oldfield, Convection-enhanced delivery of macromolecules in the brain, Proc. Natl. Acad. Sci. 91 (6) (1994) 2076–2080.
[29] N.A. de Vries, J.H. Beijnen, W. Boogerd, O. van Tellingen, Blood–brain barrier and chemotherapeutic treatment of brain tumors, Expert Rev. Neurother. 6 (8) (2006) 1199–1209.
[30] M.L. Brady, R. Raghavan, A. Alexander, K. Kubota, K. Sillay, M.E. Emborg, Pathways of Infusate loss during convection-enhanced delivery into the putamen nucleus, Stereotact. Funct. Neurosurg. 91 (2) (2013) 69–78.
[31] A.M. Mehta, A.M. Sonabend, J.N. Bruce, Convection-enhanced delivery, Neurotherapeutics. 14 (2) (2017) 358–371.
[32] R.C.E. Anderson, B. Kennedy, C.L. Yanes, J. Garvin, M. Needle, P. Canoll, et al., Convection-enhanced delivery of topotecan into diffuse intrinsic brainstem tumors in children: report of 2 cases, J. Neurosurg. Pediatr. 11 (3) (2013) 289–295.
[33] P.J. Gaillard, C.C.M. Appeldoorn, R. Dorland, J. van Kregten, F. Manca, D. J. Vugts, et al., Pharmacokinetics, Brain Delivery, and Efficacy in Brain Tumor-Bearing Mice of Glutathione Pegylated Liposomal Doxorubicin (2B3–101). Velasco G, editor, PLoS ONE 9 (1) (2014) e82331.
[34] D. Bobo, K.J. Robinson, J. Islam, K.J. Thurecht, S.R. Corrie, Nanoparticle-based medicines: a review of FDA-approved materials and clinical trials to date, Pharm. Res. 33 (10) (2016) 2373–2387.
[35] T.M. Allen, P.R. Cullis, Drug delivery systems: entering the mainstream, Science. 303 (5665) (2004) 1818–1822.
[36] C.D. Arvanitis, G.B. Ferraro, R.K. Jain, The blood–brain barrier and blood–tumour barrier in brain tumours and metastases, Nat. Rev. Cancer 20 (1) (2020) 26–41.
[37] A.B. Etame, R.J. Diaz, M.A. O'Reilly, C.A. Smith, T.G. Mainprize, K. Hynynen, et al., Enhanced delivery of gold nanoparticles with therapeutic potential into the brain using MRI-guided focused ultrasound, Nanomedicine Nanotechnol Biol Med. 8 (7) (2012) 1133–1142.
[38] A.J. Sawyer, J.K. Saucier-Sawyer, C.J. Booth, J. Liu, T. Patel, J.M. Piepmeier, et al., Convection-enhanced delivery of camptothecin-loaded polymer nanoparticles for treatment of intracranial tumors, Drug Deliv. Transl. Res. 1 (1) (2011) 34–42.
[39] B. Erdlenbruch, C. Schinkhof, W. Kugler, D.E.H. Heinemann, J. Herms, H. Eibl, et al., Intracarotid administration of short-chain alkylglycerols for increased delivery of methotrexate to the rat brain, Br. J. Pharmacol. 139 (4) (2003) 685–694.
[40] R.T. Bartus, P. Elliott, N. Hayward, R. Dean, E.L. McEwen, S.K. Fisher, Permeability of the blood brain barrier by the bradykinin agonist, RMP-7: evidence for a sensitive, auto-regulated, receptor-mediated system, Immunopharmacology. 33 (1–3) (1996) 270–278.
[41] M.D. Prados, S.C. Schold, H.A. Fine, K. Jaeckle, F. Hochberg, L. Mechtler, et al., A randomized, double-blind, placebo-controlled, phase 2 study of RMP-7 incombination with carboplatin administered intravenously for the treatment ofrecurrent malignant glioma, Neuro-Oncol. 5 (2) (2003) 96–103.
[42] W.M. Pardridge, The blood-brain barrier: bottleneck in brain drug development, NeuroRX. 2 (1) (2005) 3–14.
[43] Q.R. Smith, Y.Z. Ziylan, P.J. Robinson, S.I. Rapoport, Kinetics and distribution volumes for tracers of different sizes in the brain plasma space, Brain Res. 462 (1) (1988) 1–9.
[44] W.A. Banks, From blood–brain barrier to blood–brain interface: new opportunities for CNS drug delivery, Nat. Rev. Drug Discov. 15 (4) (2016) 275–292.
[45] B.T. Hawkins, T.P. Davis, The blood-brain barrier/neurovascular unit in health and disease, Pharmacol. Rev. 57 (2) (2005) 173–185.
[46] T.M. Mathiisen, K.P. Lehre, N.C. Danbolt, O.P. Ottersen, The perivascular astroglial sheath provides a complete covering of the brain microvessels: an electron microscopic 3D reconstruction, Glia. 58 (9) (2010) 1094–1103.
[47] J. Bart, H.J.M. Groen, N.H. Hendrikse, W.T.A. van der Graaf, W. Vaalburg, E.G. E. de Vries, The blood-brain barrier and oncology: new insights into function and modulation, Cancer Treat. Rev. 26 (6) (2000) 449–462.

[48] U.H. Langen, S. Ayloo, C. Gu, Development and cell biology of the blood-brain barrier, Annu. Rev. Cell Dev. Biol. 35 (1) (2019) 591–613.
[49] S. Banerjee, M.A. Bhat, Neuron-glial interactions in blood-brain barrier formation, Annu. Rev. Neurosci. 30 (1) (2007) 235–258.
[50] W. Löscher, H. Potschka, Drug resistance in brain diseases and the role of drug efflux transporters, Nat. Rev. Neurosci. 6 (8) (2005) 591–602.
[51] N.A. Charles, E.C. Holland, R. Gilbertson, R. Glass, H. Kettenmann, The brain tumor microenvironment, Glia. 59 (8) (2011) 1169–1180.
[52] B. Engelhardt, S. Liebner, Novel insights into the development and maintenance of the blood–brain barrier, Cell Tissue Res. 355 (3) (2014) 687–699.
[53] H.J. Scherer, The forms of growth in gliomas and their practical significance, Brain. 63 (1) (1940) 1–35.
[54] C. Chaves, X. Declèves, M. Taghi, M.C. Menet, J. Lacombe, P. Varlet, et al., Characterization of the blood–brain barrier integrity and the brain transport of SN-38 in an orthotopic xenograft rat model of diffuse intrinsic pontine glioma, Pharmaceutics 12 (5) (2020) 399.
[55] D. Gomez-Zepeda, M. Taghi, J.M. Scherrmann, X. Decleves, M.C. Menet, ABC transporters at the blood–brain interfaces, their study models, and drug delivery implications in gliomas, Pharmaceutics. 12 (1) (2019) 20.
[56] C. Deligne, J. Hachani, S. Duban-Deweer, S. Meignan, P. Leblond, A. M. Carcaboso, et al., Development of a human in vitro blood–brain tumor barrier model of diffuse intrinsic pontine glioma to better understand the chemoresistance, Fluids Barriers CNS. 17 (1) (2020) 37.
[57] K.E. Warren, Beyond the Blood: Brain Barrier: The Importance of Central Nervous System (CNS) Pharmacokinetics for the Treatment of CNS Tumors, Including Diffuse Intrinsic Pontine Glioma, Front. Oncol. 3 (8) (2018) 239.
[58] C.M. McCully, D. Pastakia, J. Bacher, E.A. Steffen-Smith, K. Saleem, R.F. Murphy, et al., Model for concomitant microdialysis sampling of the pons and cerebral cortex in rhesus macaques (Macaca mulatta), Comp. Med. 63 (4) (2013) 355–360.
[59] C. Chapouly, S. Guimbal, P.L. Hollier, M.A. Renault, Role of hedgehog signaling in vasculature development, differentiation, and maintenance, Int. J. Mol. Sci. 20 (12) (2019) 3076.
[60] S.J.E. Veringa, D. Biesmans, D.G. van Vuurden, M.H.A. Jansen, L.E. Wedekind, I. Horsman, et al., In Vitro Drug Response and Efflux Transporters Associated with Drug Resistance in Pediatric high grade glioma and diffuse intrinsic pontine glioma. Ulasov I, editor, PLoS ONE 8 (4) (2013) e61512.
[61] M. Bredel, J. Zentner, Brain-tumour drug resistance: the bare essentials, Lancet Oncol. 3 (7) (2002) 397–406.
[62] K. Hynynen, N. McDannold, N. Vykhodtseva, F.A. Jolesz, Noninvasive MR imaging–guided focal opening of the blood-brain barrier in rabbits, Radiology. 220 (3) (2001) 640–646.
[63] N. McDannold, C.D. Arvanitis, N. Vykhodtseva, M.S. Livingstone, Temporary disruption of the blood–brain barrier by use of ultrasound and microbubbles: safety and efficacy evaluation in rhesus macaquesblood–brain barrier disruption via focused ultrasound, Cancer Res. 72 (14) (2012) 3652–3663.
[64] H.L. Liu, M.Y. Hua, P.Y. Chen, P.C. Chu, C.H. Pan, H.W. Yang, et al., Blood-brain barrier disruption with focused ultrasound enhances delivery of chemotherapeutic drugs for glioblastoma treatment, Radiology. 255 (2) (2010) 415–425.
[65] K.H. Song, A.C. Fan, J.J. Hinkle, J. Newman, M.A. Borden, B.K. Harvey, Microbubble gas volume: a unifying dose parameter in blood-brain barrier opening by focused ultrasound, Theranostics. 7 (1) (2017) 144–152.
[66] M.A. Borden, K.H. Song, Reverse engineering the ultrasound contrast agent, Adv. Colloid Interface Sci. 262 (2018) 39–49.
[67] P. Frinking, T. Segers, Y. Luan, F. Tranquart, Three decades of ultrasound contrast agents: a review of the past, present and future improvements, Ultrasound Med. Biol. 46 (4) (2020) 892–908.
[68] E. Stride, T. Segers, G. Lajoinie, S. Cherkaoui, T. Bettinger, M. Versluis, et al., Microbubble agents: new directions, Ultrasound Med. Biol. 46 (6) (2020) 1326–1343.
[69] A. Dasgupta, M. Liu, T. Ojha, G. Storm, F. Kiessling, T. Lammers, Ultrasound-mediated drug delivery to the brain: principles, progress and prospects, Drug Discov. Today Technol. 20 (2016) 41–48.
[70] K.H. Song, B.K. Harvey, M.A. Borden, State-of-the-art of microbubble-assisted blood-brain barrier disruption, Theranostics. 8 (16) (2018) 4393–4408.
[71] P. Martinez, N. Bottenus, M. Borden, Cavitation characterization of size-isolated microbubbles in a vessel phantom using focused ultrasound, Pharmaceutics. 14 (9) (2022) 1925.
[72] I. Lentacker, I. De Cock, R. Deckers, S.C. De Smedt, C.T.W. Moonen, Understanding ultrasound induced sonoporation: definitions and underlying mechanisms, Adv. Drug Deliv. Rev. 72 (2014) 49–64.
[73] E. Konofagou, Y.S. Tunga, J. Choia, T. Deffieuxa, B. Baseria, F. Vlachosa, Ultrasound-induced blood-brain barrier opening, Curr. Pharm. Biotechnol. 13 (7) (2012) 1332–1345.
[74] Z.I. Kovacs, S. Kim, N. Jikaria, F. Qureshi, B. Milo, B.K. Lewis, et al., Disrupting the blood–brain barrier by focused ultrasound induces sterile inflammation, Proc Natl Acad Sci 114 (1) (2017) E75–E84, 3 [cited 2022 5]. Available from: https://pnas.org/doi/full/10.1073/pnas.1614777114.
[75] J.B. Joiner, Y. Pylayeva-Gupta, P.A. Dayton, Focused ultrasound for immunomodulation of the tumor microenvironment, J. Immunol. 205 (9) (2020) 2327–2341.
[76] S. Liebner, R.M. Dijkhuizen, Y. Reiss, K.H. Plate, D. Agalliu, G. Constantin, Functional morphology of the blood–brain barrier in health and disease, Acta Neuropathol (Berl). 135 (3) (2018) 311–336.
[77] M. Aryal, K. Fischer, C. Gentile, S. Gitto, Y.Z. Zhang, N. McDannold, Effects on P-glycoprotein expression after blood-brain barrier disruption using focused ultrasound and microbubbles. Toborek M, editor, PLOS ONE 12 (1) (2017) e0166061.
[78] H. Cho, H.Y. Lee, M. Han, J. Choi, S. Ahn, T. Lee, et al., Localized Down-regulation of P-glycoprotein by focused ultrasound and microbubbles induced blood-brain barrier disruption in rat brain, Sci. Rep. 6 (1) (2016) 31201.
[79] S. Alli, C.A. Figueiredo, B. Golbourn, N. Sabha, M.Y. Wu, A. Bondoc, et al., Brainstem blood brain barrier disruption using focused ultrasound: a demonstration of feasibility and enhanced doxorubicin delivery, J. Control. Release 281 (2018) 29–41.
[80] D. Ye, D. Sultan, X. Zhang, Y. Yue, G.S. Heo, S.V.V.N. Kothapalli, et al., Focused ultrasound-enabled delivery of radiolabeled nanoclusters to the pons, J. Control. Release 283 (2018) 143–150.
[81] J. Ishida, S. Alli, A. Bondoc, B. Golbourn, N. Sabha, K. Mikloska, et al., MRI-guided focused ultrasound enhances drug delivery in experimental diffuse intrinsic pontine glioma, J. Control. Release 330 (2021) 1034–1045.
[82] Z.K. Englander, H.J. Wei, A.N. Pouliopoulos, E. Bendau, P. Upadhyayula, C.I. Jan, et al., Focused ultrasound mediated blood–brain barrier opening is safe and feasible in a murine pontine glioma model, Sci. Rep. 11 (1) (2021) 6521.
[83] R. Haumann, J.I. Bianco, P.M. Waranecki, P.J. Gaillard, G. Storm, M. Ries, et al., Imaged-guided focused ultrasound in combination with various formulations of doxorubicin for the treatment of diffuse intrinsic pontine glioma, Transl Med Commun. 7 (1) (2022) 1–12.
[84] P. Martinez, G. Nault, J. Steiner, M.F. Wempe, A. Pierce, B. Brunt, et al., MRI-guided focused ultrasound blood–brain barrier opening increases drug delivery and efficacy in a diffuse midline glioma mouse model, Neuro-Oncol Adv. 5 (1) (2023) vdad111.
[85] C.Y. Ting, C.H. Fan, H.L. Liu, C.Y. Huang, H.Y. Hsieh, T.C. Yen, et al., Concurrent blood–brain barrier opening and local drug delivery using drug-carrying microbubbles and focused ultrasound for brain glioma treatment, Biomaterials. 33 (2) (2012) 704–712.
[86] C.H. Fan, C.Y. Ting, H.L. Liu, C.Y. Huang, H.Y. Hsieh, T.C. Yen, et al., Antiangiogenic-targeting drug-loaded microbubbles combined with focused ultrasound for glioma treatment, Biomaterials. 34 (8) (2013) 2142–2155.
[87] C.H. Fan, C.Y. Ting, Y.C. Chang, K.C. Wei, H.L. Liu, C.K. Yeh, Drug-loaded bubbles with matched focused ultrasound excitation for concurrent blood–brain barrier opening and brain-tumor drug delivery, Acta Biomater. 15 (2015) 89–101.
[88] H.J. Wei, A. Pouliopoulos, N. Yoh, M. Tazhibi, N. McQuillan, X. Zhang, et al., Focused ultrasound-mediated blood-brain barrier opening enhances Panobinostat efficacy in a murine diffuse intrinsic pontine glioma model, Int J Radiat Oncol. 111 (3) (2021), e177.
[89] H.J. Wei, P.S. Upadhyayula, A.N. Pouliopoulos, Z.K. Englander, X. Zhang, C. I. Jan, et al., Focused ultrasound-mediated blood-brain barrier opening increases delivery and efficacy of etoposide for glioblastoma treatment, Int J Radiat Oncol. 110 (2) (2021) 539–550.
[90] N. McDannold, Y. Zhang, J.G. Supko, C. Power, T. Sun, N. Vykhodtseva, et al., Blood-brain barrier disruption and delivery of irinotecan in a rat model using a clinical transcranial MRI-guided focused ultrasound system, Sci. Rep. 10 (1) (2020) 8766.
[91] N. McDannold, Y. Zhang, J.G. Supko, C. Power, T. Sun, C. Peng, et al., Acoustic feedback enables safe and reliable carboplatin delivery across the blood-brain barrier with a clinical focused ultrasound system and improves survival in a rat glioma model, Theranostics. 9 (21) (2019) 6284–6299.
[92] L.H. Treat, N. McDannold, Y. Zhang, N. Vykhodtseva, K. Hynynen, Improved anti-tumor effect of liposomal doxorubicin after targeted blood-brain barrier disruption by MRI-guided focused ultrasound in rat glioma, Ultrasound Med. Biol. 38 (10) (2012) 1716–1725.
[93] Z. Kovacs, B. Werner, A. Rassi, J.O. Sass, E. Martin-Fiori, M. Bernasconi, Prolonged survival upon ultrasound-enhanced doxorubicin delivery in two syngenic glioblastoma mouse models, J. Control. Release 187 (2014) 74–82.
[94] J. Park, M. Aryal, N. Vykhodtseva, Y.Z. Zhang, N. McDannold, Evaluation of permeability, doxorubicin delivery, and drug retention in a rat brain tumor model after ultrasound-induced blood-tumor barrier disruption, J. Control. Release 250 (2017) 77–85.
[95] Y.L. Lin, M.T. Wu, F.Y. Yang, Pharmacokinetics of doxorubicin in glioblastoma multiforme following ultrasound-induced blood-brain barrier disruption as determined by microdialysis, J. Pharm. Biomed. Anal. 149 (2018) 482–487.
[96] T. Kobus, I.K. Zervantonakis, Y. Zhang, N.J. McDannold, Growth inhibition in a brain metastasis model by antibody delivery using focused ultrasound-mediated blood-brain barrier disruption, J. Control. Release 238 (2016) 281–288.
[97] E.J. Park, Y.Z. Zhang, N. Vykhodtseva, N. McDannold, Ultrasound-mediated blood-brain/blood-tumor barrier disruption improves outcomes with trastuzumab in a breast cancer brain metastasis model, J. Control. Release 163 (3) (2012) 277–284.
[98] M. Kinoshita, N. McDannold, F.A. Jolesz, K. Hynynen, Noninvasive localized delivery of Herceptin to the mouse brain by MRI-guided focused ultrasound-induced blood–brain barrier disruption, Proc. Natl. Acad. Sci. 103 (31) (2006) 11719–11723.
[99] K.F. Timbie, B.P. Mead, R.J. Price, Drug and gene delivery across the blood–brain barrier with focused ultrasound, J. Control. Release 219 (2015) 61–75.
[100] P.Y. Chen, H.Y. Hsieh, C.Y. Huang, C.Y. Lin, K.C. Wei, H.L. Liu, Focused ultrasound-induced blood–brain barrier opening to enhance interleukin-12 delivery for brain tumor immunotherapy: a preclinical feasibility study, J. Transl. Med. 13 (1) (2015) 93.

[101] H.L. Liu, P.H. Hsu, C.Y. Lin, C.W. Huang, W.Y. Chai, P.C. Chu, et al., Focused ultrasound enhances central nervous system delivery of bevacizumab for malignant glioma treatment, Radiology. 281 (1) (2016) 99–108.
[102] S. Syvänen, J. Eriksson, Advances in PET imaging of P-glycoprotein function at the blood-brain barrier, ACS Chem. Nerosci. 4 (2) (2013) 225–237.
[103] W.M. Arif, P.H. Elsinga, C. Gasca-Salas, M. Versluis, R. Martínez-Fernández, R.A. J.O. Dierckx, et al., Focused ultrasound for opening blood-brain barrier and drug delivery monitored with positron emission tomography, J. Control. Release 324 (2020) 303–316.
[104] H. Chen, E.E. Konofagou, The size of blood–brain barrier opening induced by focused ultrasound is dictated by the acoustic pressure, J. Cereb. Blood Flow Metab. 34 (7) (2014) 1197–1204.
[105] J.J. Choi, S. Wang, Y.S. Tung, B. Morrison, E.E. Konofagou, Molecules of various pharmacologically-relevant sizes can cross the ultrasound-induced blood-brain barrier opening in vivo, Ultrasound Med. Biol. 36 (1) (2010) 58–67.
[106] A. Papachristodoulou, R.D. Signorell, B. Werner, D. Brambilla, P. Luciani, M. Cavusoglu, et al., Chemotherapy sensitization of glioblastoma by focused ultrasound-mediated delivery of therapeutic liposomes, J. Control. Release 295 (2019) 130–139.
[107] N.R. Saunders, K.M. Dziegielewska, K. Møllgård, M.D. Habgood, Markers for blood-brain barrier integrity: how appropriate is Evans blue in the twenty-first century and what are the alternatives? Front. Neurosci. 9 (2015) 385.
[108] N.D. Sheybani, V.R. Breza, S. Paul, K.S. McCauley, S.S. Berr, G.W. Miller, et al., ImmunoPET-informed sequence for focused ultrasound-targeted mCD47 blockade controls glioma, J. Control. Release 331 (2021) 19–29.
[109] R.J. Diaz, P.Z. McVeigh, M.A. O'Reilly, K. Burrell, M. Bebenek, C. Smith, et al., Focused ultrasound delivery of Raman nanoparticles across the blood-brain barrier: potential for targeting experimental brain tumors, Nanomedicine Nanotechnol Biol Med. 10 (5) (2014) e1075–e1087.
[110] R.D. Alkins, P.M. Brodersen, R.N.S. Sodhi, K. Hynynen, Enhancing drug delivery for boron neutron capture therapy of brain tumors with focused ultrasound, Neuro-Oncol. 15 (9) (2013) 1225–1235.
[111] D. Coluccia, C.A. Figueiredo, M.Y. Wu, A.N. Riemenschneider, R. Diaz, A. Luck, et al., Enhancing glioblastoma treatment using cisplatin-gold-nanoparticle conjugates and targeted delivery with magnetic resonance-guided focused ultrasound, Nanomedicine Nanotechnol Biol Med. 14 (4) (2018) 1137–1148.
[112] M. Aryal, J. Park, N. Vykhodtseva, Y.Z. Zhang, N. McDannold, Enhancement in blood-tumor barrier permeability and delivery of liposomal doxorubicin using focused ultrasound and microbubbles: evaluation during tumor progression in a rat glioma model, Phys. Med. Biol. 60 (6) (2015) 2511–2527.
[113] L.H. Treat, N. McDannold, N. Vykhodtseva, Y. Zhang, K. Tam, K. Hynynen, Targeted delivery of doxorubicin to the rat brain at therapeutic levels using MRI-guided focused ultrasound, Int. J. Cancer 121 (4) (2007) 901–907.
[114] H. Breuer, M. Meier, S. Schneefeld, W. Härtig, A. Wittneben, M. Märkel, et al., Multimodality imaging of blood–brain barrier impairment during epileptogenesis, J. Cereb. Blood Flow Metab. 37 (6) (2017) 2049–2061.
[115] R. Gilad, Y. Lampl, A. Eilam, M. Boaz, M. Loyberboim, SPECT-DTPA as a tool for evaluating the blood–brain barrier in post-stroke seizures, J. Neurol. 259 (10) (2012) 2041–2044.
[116] F.Y. Yang, W.Y. Chang, J.C. Chen, L.C. Lee, Y.S. Hung, Quantitative assessment of cerebral glucose metabolic rates after blood–brain barrier disruption induced by focused ultrasound using FDG-MicroPET, NeuroImage. 90 (2014) 93–98.
[117] H. Kim, M. Park, S. Wang, A. Chiu, K. Fischer, S. Yoo, PET/CT imaging evidence of FUS-mediated (18)F-FDG uptake changes in rat brain, Med. Phys. 40 (3) (2013), 033501.
[118] S.S. Zoghbi, J.S. Liow, F. Yasuno, J. Hong, E. Tuan, N. Lazarova, et al., ^{11}C-Loperamide and its *N - Desmethyl* Radiometabolite are avid substrates for brain permeability-glycoprotein efflux, J. Nucl. Med. 49 (4) (2008) 649–656.
[119] S. Goutal, M. Gerstenmayer, S. Auvity, F. Caillé, S. Mériaux, I. Buvat, et al., Physical blood-brain barrier disruption induced by focused ultrasound does not overcome the transporter-mediated efflux of erlotinib, J. Control. Release 292 (2018) 210–220.
[120] M.D. Sweeney, A.P. Sagare, B.V. Zlokovic, Blood–brain barrier breakdown in Alzheimer disease and other neurodegenerative disorders, Nat. Rev. Neurol. 14 (3) (2018) 133–150.
[121] G. Luurtsema, C.F.M. Molthoff, R.C. Schuit, A.D. Windhorst, A.A. Lammertsma, E. J.F. Franssen, Evaluation of (R)-[11C]verapamil as PET tracer of P-glycoprotein function in the blood–brain barrier: kinetics and metabolism in the rat, Nucl. Med. Biol. 32 (1) (2005) 87–93.
[122] L. García-Varela, D.V. García, T. Kakiuchi, H. Ohba, S. Nishiyama, T. Tago, et al., Pharmacokinetic modeling of (*R*)-[^{11}C]verapamil to measure the P-glycoprotein function in nonhuman primates, Mol. Pharm. 18 (1) (2021) 416–428.
[123] S. Goutal, A. Novell, S. Leterrier, L. Breuil, E. Selingue, M. Gerstenmayer, et al., Imaging the impact of blood-brain barrier disruption induced by focused ultrasound on P-glycoprotein function, J. Control. Release 361 (2023) 483–492.
[124] K.C. Wei, P.C. Chu, H.Y.J. Wang, C.Y. Huang, P.Y. Chen, H.C. Tsai, et al., Focused ultrasound-induced blood–brain barrier opening to enhance temozolomide delivery for glioblastoma treatment: a preclinical study. He X, editor, PLoS ONE 8 (3) (2013) e58995.
[125] H.L. Liu, C.Y. Huang, J.Y. Chen, H.Y.J. Wang, P.Y. Chen, K.C. Wei, Pharmacodynamic and therapeutic investigation of focused ultrasound-induced blood-brain barrier opening for enhanced temozolomide delivery in glioma treatment. He X, editor, PLoS ONE 9 (12) (2014) e114311.
[126] Y. Shen, Z. Pi, F. Yan, C.K. Yeh, X. Zeng, X. Diao, et al., Enhanced delivery of paclitaxel liposomes using focused ultrasound with microbubbles for treating nude mice bearing intracranial glioblastoma xenografts, Int. J. Nanomedicine 12 (2017) 5613–5629.
[127] N. McDannold, N. Vykhodtseva, K. Hynynen, Blood-brain barrier disruption induced by focused ultrasound and circulating preformed microbubbles appears to be characterized by the mechanical index, Ultrasound Med. Biol. 34 (5) (2008) 834–840.
[128] R.E. Apfel, C.K. Holland, Gauging the likelihood of cavitation from short-pulse, low-duty cycle diagnostic ultrasound, Ultrasound Med. Biol. 17 (2) (1991) 179–185.
[130] N. McDannold, N. Vykhodtseva, K. Hynynen, Effects of acoustic parameters and ultrasound contrast agent dose on focused-ultrasound induced blood-brain barrier disruption, Ultrasound Med. Biol. 34 (6) (2008) 930–937.
[131] C.D. Arvanitis, M.S. Livingstone, N. Vykhodtseva, N. McDannold, Controlled ultrasound-induced blood-brain barrier disruption using passive acoustic emissions monitoring, PLOS ONE 7 (9) (2021) e45783, https://doi.org/10.1371/journal.pone.0045783.
[132] A.N. Pouliopoulos, N. Kwon, G. Jensen, A. Meaney, Y. Niimi, M.T. Burgess, et al., Safety evaluation of a clinical focused ultrasound system for neuronavigation guided blood-brain barrier opening in non-human primates, Sci. Rep. 11 (1) (2021) 15043.
[133] F. Marquet, T. Teichert, V. Ferrera, E.E. Konofagou, Feasibility of noninvasive cavitation-guided blood-brain barrier opening using focused ultrasound and microbubbles in nonhuman primates, Appl. Phys. Lett. 98 (16) (2011), 163704.
[134] J.J. Choi, K. Selert, Z. Gao, G. Samiotaki, B. Baseri, E.E. Konofagou, Noninvasive and localized blood—brain barrier disruption using focused ultrasound can be achieved at short pulse lengths and low pulse repetition frequencies, J. Cereb. Blood Flow Metab. 31 (2) (2011) 725–737.
[135] S.V. Morse, A.N. Pouliopoulos, T.G. Chan, M.J. Copping, J. Lin, N.J. Long, et al., Rapid short-pulse ultrasound delivers drugs uniformly across the murine blood-brain barrier with negligible disruption, Radiology. 291 (2) (2019) 459–466.
[136] S.V. Morse, A. Mishra, T.G. Chan, T.M. De Rosales, J.J. Choi, Liposome delivery to the brain with rapid short-pulses of focused ultrasound and microbubbles, J. Control. Release 341 (2022) 605–615.
[137] W. Lim Kee Chang, T.G. Chan, F. Raguseo, A. Mishra, D. Chattenton, De Rosales RTM, et al., Rapid short-pulses of focused ultrasound and microbubbles deliver a range of agent sizes to the brain, Sci Rep. 13 (1) (2023) 6963.
[138] C. Brighi, E. Salimova, M. de Veer, S. Puttick, G. Egan, Translation of focused ultrasound for blood-brain barrier opening in glioma, J. Control. Release 345 (2022) 443–463.
[139] M.A. O'Reilly, K. Hynynen, Blood-brain barrier: real-time feedback-controlled focused ultrasound disruption by using an acoustic emissions–based controller, Radiology. 263 (1) (2012) 96–106.
[140] T. Sun, Y. Zhang, C. Power, P.M. Alexander, J.T. Sutton, M. Aryal, et al., Closed-loop control of targeted ultrasound drug delivery across the blood–brain/tumor barriers in a rat glioma model, Proc Natl Acad Sci 114 (48) (2017) E10281–E10290. Nov 28 [cited 2022 5]. Available from: https://pnas.org/doi/full/10.1073/pnas.1713328114.
[141] N. Asquier, G. Bouchoux, M. Canney, C. Martin, B. Law-Ye, D. Leclercq, et al., Blood-brain barrier disruption in humans using an implantable ultrasound device: quantification with MR images and correlation with local acoustic pressure, J. Neurosurg. 132 (3) (2020) 875–883.
[142] A. Jameel, P. Bain, D. Nandi, B. Jones, W. Gedroyc, Device profile of exAblate neuro 4000, the leading system for brain magnetic resonance guided focused ultrasound technology: an overview of its safety and efficacy in the treatment of medically refractory essential tremor, Expert Rev. Med. Devices 18 (5) (2021) 429–437.
[143] K.T. Chen, Y.J. Lin, W.Y. Chai, C.J. Lin, P.Y. Chen, C.Y. Huang, et al., Neuronavigation-guided focused ultrasound (NaviFUS) for transcranial blood-brain barrier opening in recurrent glioblastoma patients: clinical trial protocol, Ann Transl Med. 8 (11) (2020) 673.
[144] J.M. Hyvelin, E. Gaud, M. Costa, A. Helbert, P. Bussat, T. Bettinger, et al., Characteristics and echogenicity of clinical ultrasound contrast agents: an in vitro and in vivo comparison study: comparison of clinical ultrasound contrast agents, J. Ultrasound Med. 36 (5) (2017) 941–953.
[145] D. McMahon, K. Hynynen, Acute inflammatory response following increased blood-brain barrier permeability induced by focused ultrasound is dependent on microbubble dose, Theranostics. 7 (16) (2017) 3989–4000.
[146] Z. Pi, Y. Huang, Y. Shen, X. Zeng, Y. Hu, T. Chen, et al., Sonodynamic therapy on intracranial glioblastoma xenografts using Sinoporphyrin sodium delivered by ultrasound with microbubbles, Ann. Biomed. Eng. 47 (2) (2019) 549–562.
[147] D. Ye, J. Yuan, Y. Yue, J.B. Rubin, H. Chen, Focused ultrasound-enhanced delivery of Intranasally administered anti-programmed cell death-ligand 1 antibody to an intracranial murine glioma model, Pharmaceutics. 13 (2) (2021) 190.
[148] G. Zhao, Q. Huang, F. Wang, X. Zhang, J. Hu, Y. Tan, et al., Targeted shRNA-loaded liposome complex combined with focused ultrasound for blood brain barrier disruption and suppressing glioma growth, Cancer Lett. 418 (2018) 147–158.
[149] C.H. Fan, C.Y. Ting, H.J. Lin, C.H. Wang, H.L. Liu, T.C. Yen, et al., SPIO-conjugated, doxorubicin-loaded microbubbles for concurrent MRI and focused-ultrasound enhanced brain-tumor drug delivery, Biomaterials. 34 (14) (2013) 3706–3715.
[150] C.H. Fan, Y.H. Cheng, C.Y. Ting, Y.J. Ho, P.H. Hsu, H.L. Liu, et al., Ultrasound/magnetic targeting with SPIO-DOX-microbubble complex for image-guided drug delivery in brain tumors, Theranostics. 6 (10) (2016) 1542–1556.

[151] J.A. Navarro-Becerra, J.I. Castillo, F. Di Ruzza, M.A. Borden, Monodispersity increases adhesion efficiency and specificity for ultrasound-targeted microbubbles, ACS Biomater Sci. Eng. 9 (2) (2022) 991–1001.
[152] C. Bing, Y. Hong, C. Hernandez, M. Rich, B. Cheng, I. Munaweera, et al., Characterization of different bubble formulations for blood-brain barrier opening using a focused ultrasound system with acoustic feedback control, Sci. Rep. 8 (1) (2018) 7986.
[153] A. Dauba, A. Delalande, H.A.S. Kamimura, A. Conti, B. Larrat, N. Tsapis, et al., Recent advances on ultrasound contrast agents for blood-brain barrier opening with focused ultrasound, Pharmaceutics. 12 (11) (2020) 1125.
[154] B.L. Helfield, X. Huo, R. Williams, D.E. Goertz, The effect of Preactivation vial temperature on the acoustic properties of DefinityTM, Ultrasound Med. Biol. 38 (7) (2012) 1298–1305.
[155] S.Y. Wu, C.S. Sanchez, G. Samiotaki, A. Buch, V.P. Ferrera, E.E. Konofagou, Characterizing focused-ultrasound mediated drug delivery to the heterogeneous primate brain in vivo with acoustic monitoring, Sci. Rep. 6 (1) (2016) 37094.